

# SOLITON DYNAMICS IN 3D FERROMAGNETS

Theodora Ioannidou and Paul M. Sutcliffe

*Institute of Mathematics, University of Kent at Canterbury,*

*Canterbury, CT2 7NF, U.K.*

*Email : T.Ioannidou@ukc.ac.uk*

*Email : P.M.Sutcliffe@ukc.ac.uk*

November 2000

## **Abstract**

We study the dynamics of solitons in a Landau-Lifshitz equation describing the magnetization of a three-dimensional ferromagnet with an easy axis anisotropy. We numerically compute the energy dispersion relation and the structure of moving solitons, using a constrained minimization algorithm. We compare the results with those obtained using an approximate form for the moving soliton, valid in the small momentum limit. We also study the interaction and scattering of two solitons, through a numerical simulation of the (3+1)-dimensional equations of motion. We find that the force between two solitons can be either attractive or repulsive depending on their relative internal phase and that in a collision two solitons can form an unstable oscillating loop of magnons.

# 1 Introduction

In the continuum approximation the state of a ferromagnet is described by a three component unit vector,  $\boldsymbol{\phi}(\mathbf{x}, t)$ , which gives the local orientation of the magnetization. The dynamics of the ferromagnet, in the absence of dissipation, is governed by the Landau-Lifshitz equation

$$\frac{\partial \boldsymbol{\phi}}{\partial t} = -\boldsymbol{\phi} \times \frac{\delta E}{\delta \boldsymbol{\phi}} \quad (1.1)$$

where  $E$  is the magnetic crystal energy of the ferromagnet. We have chosen units in which the spin stiffness and magnetic moment density of the ferromagnet are set to one.

The case we study in this paper is that of a three-dimensional ferromagnet with isotropic exchange interactions and an easy-axis anisotropy, in which case the energy is given by

$$E = \frac{1}{2} \int (\partial_i \boldsymbol{\phi} \cdot \partial_i \boldsymbol{\phi} + A(1 - \phi_3^2)) d^3 \mathbf{x} \quad (1.2)$$

where  $A > 0$  is the anisotropy parameter and we choose the ground state to be  $\boldsymbol{\phi} = (\phi_1, \phi_2, \phi_3) = (0, 0, 1) = \mathbf{e}_3$ .

In this case the Landau-Lifshitz equation becomes

$$\frac{\partial \boldsymbol{\phi}}{\partial t} = \boldsymbol{\phi} \times (\partial_i \partial_i \boldsymbol{\phi} + A \phi_3 \mathbf{e}_3). \quad (1.3)$$

This equation has finite energy, stable, exponentially localized solutions known as magnetic solitons [5]. In section 2 we review the properties of stationary magnetic solitons and in section 3 we numerically compute solutions describing moving solitons, display their energy dispersion relation and discuss their structure. Finally, in section 4, we perform numerical simulations of the time dependent equations of motion to investigate the interaction and scattering of two solitons. We find that the force between two solitons depends on their relative internal phase, and that during a collision two solitons can form an unstable loop of magnons which subsequently decays into solitons.

## 2 Stationary Solitons

In addition to the energy (1.2), the Landau-Lifshitz equation (1.3) has two other conserved quantities. These are the number of spin reversals,  $N$ , and the momentum  $\mathbf{P}$ , given by [6]

$$N = \int (1 - \phi_3) d^3 \mathbf{x} \quad (2.1)$$

and

$$P_i = \frac{1}{4} \epsilon_{ijk} \int x_j \epsilon_{klm} \boldsymbol{\phi} \cdot \partial_l \boldsymbol{\phi} \times \partial_m \boldsymbol{\phi} d^3 \mathbf{x}. \quad (2.2)$$

In the quantum description,  $N$  counts the number of quasi-particles in the magnet, that is, it may be interpreted as the magnon number.

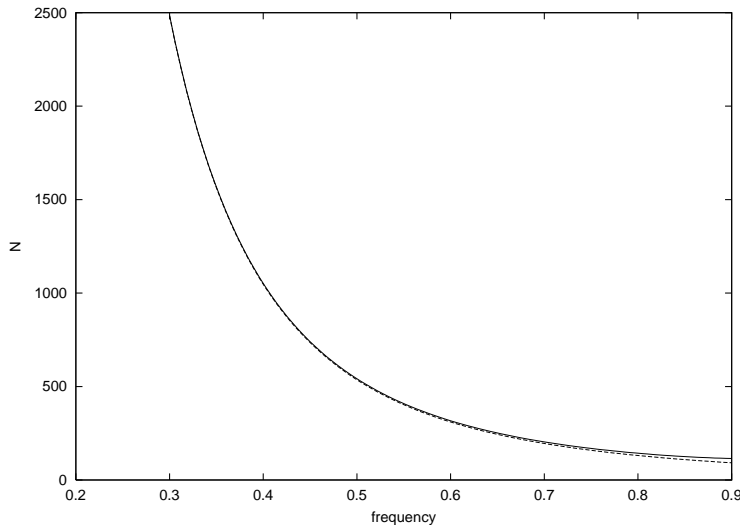


Figure 1: The number of spin reversals,  $N$ , as a function of the precession frequency  $\omega$ . The solid curve is the numerical result and the dashed curve is the approximate formula (2.6).

In this section we consider only stationary solitons, ie  $\mathbf{P} = 0$ , whose properties have been discussed in ref.[5]. There are no static solitons, but stationary solitons have a time dependence which resides only in the constant motion of an internal phase. Explicitly, the stationary soliton has the form

$$\phi = \frac{1}{1+f^2}(2f \cos(\omega t), -2f \sin(\omega t), 1-f^2) \quad (2.3)$$

where  $\omega$  is the frequency and  $f(r)$  is a real profile function with the boundary conditions  $f(\infty) = 0$ ,  $f'(0) = 0$ . The resulting equation for the profile function is

$$f'' = -\frac{2f'}{r} + \frac{2ff'' + Af(1-f^2)}{1+f^2} - \omega f \quad (2.4)$$

For large  $r$  this equation may be linearized to give the asymptotic solution

$$f \sim B \exp(-r\sqrt{A-\omega}) \quad (2.5)$$

from which it can be seen that a soliton solution exists only for  $\omega < A$ . It can also be shown that  $\omega > 0$  and hence an anisotropy term is vital for the existence of these stationary solitons. From now on we set  $A = 1$  so that  $0 < \omega < 1$ . There is a one-parameter family of stationary solitons parameterized by either the frequency  $\omega$  or the number of spin reversals  $N$ . In figure 1 we plot the relation between these two quantities, obtained by solving equation (2.4) using a shooting method (solid curve), and in figure 2 we display (solid curve) the energy per spin reversal of the soliton,  $E/N$  as a function of  $N$ .

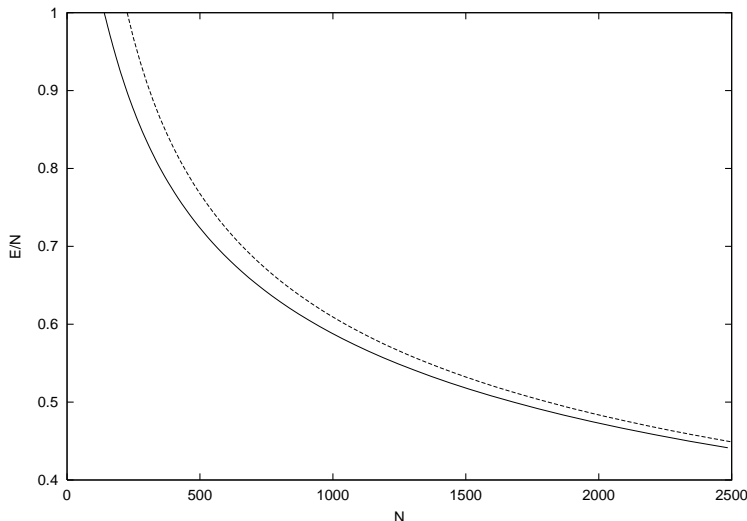


Figure 2: The energy per spin reversal,  $E/N$ , as a function of the spin reversal  $N$ . The solid curve is the numerical result and the dashed curve is the approximate formula (2.6).

In the limit of small  $\omega$  (which corresponds to large  $N$ ) the solution is approximately given by  $f = e^{R-r}$ , where  $R \gg 1$  is a core radius which marks the boundary between the two vacua  $\phi = \pm \mathbf{e}_3$  inside and outside the soliton. In this case the soliton may be thought of as a spherical domain wall. Using this simple approximate solution the following asymptotic formula may be derived, which are valid for large  $N$

$$N = \frac{64\pi}{3\omega^3}, \quad E = \frac{32\pi}{\omega^2} = (72\pi N^2)^{1/3}. \quad (2.6)$$

The dashed curves in figures 1 and 2 are obtained from these asymptotic formulae and fit the numerical results well.

### 3 Moving Solitons

To compute moving solitons is a more difficult task than in the stationary case and can not be reduced to simply solving an ordinary differential equation. There is an ansatz which is consistent with the equations of motion and describes a soliton which moves at constant velocity  $\mathbf{v}$  and rotates in internal space with frequency  $\omega$ . Explicitly the ansatz reads

$$\phi_1 + i\phi_2 = (\hat{\phi}_1(\mathbf{x} - \mathbf{v}t) + i\hat{\phi}_2(\mathbf{x} - \mathbf{v}t))e^{-i\omega t}, \quad \phi_3 = \hat{\phi}_3(\mathbf{x} - \mathbf{v}t). \quad (3.1)$$

Substituting this ansatz into the equation of motion (1.3) leads to a partial differential equation for  $\hat{\phi}$  which is not compatible with a spherically symmetric solution for non-zero  $\mathbf{v}$ . This partial differential equation has a variational formulation, which is useful

in computing its solutions. Let  $\hat{E}(\mathbf{P}, N)$  be the minimal value of  $E$  for fixed values of the momentum  $\mathbf{P}$  and number of spin reversals  $N$ . Then the solution of this constrained minimization problem is precisely the function  $\hat{\phi}$  corresponding to the values [8]

$$\omega = \left. \frac{\partial \hat{E}}{\partial N} \right|_{\mathbf{P}}, \quad v_i = \left. \frac{\partial \hat{E}}{\partial P_i} \right|_N. \quad (3.2)$$

We compute moving soliton solutions by numerically solving this constrained minimization problem. A similar computation has been performed in the case of an isotropic magnet ( $A = 0$ ) [3], but the results in this case are qualitatively different. For example, we have already seen that without anisotropy there are no stationary solutions, and in fact moving solitons exist in the isotropic case only for sufficiently large momenta [3].

A moving soliton has an axial symmetry in the plane perpendicular to its momentum  $\mathbf{P}$ . Since the Landau-Lifshitz equation is  $SO(3)$  invariant we can, without loss of generality, choose the momentum to be in the  $x_3$  direction,  $\mathbf{P} = (0, 0, P)$ , so that the soliton moves along the  $x_3$  axis and has an axial symmetry in the  $x_1x_2$  plane. We use cylindrical coordinates, with  $\rho = \sqrt{x_1^2 + x_2^2}$ , and discretize the energy using second order differences and a grid of size  $50 \times 100$  in the  $\rho, x_3$  plane. The energy is minimized using a simulated annealing algorithm [9, 4] and the constraints on  $N$  and  $P$  are imposed using a penalty function method.

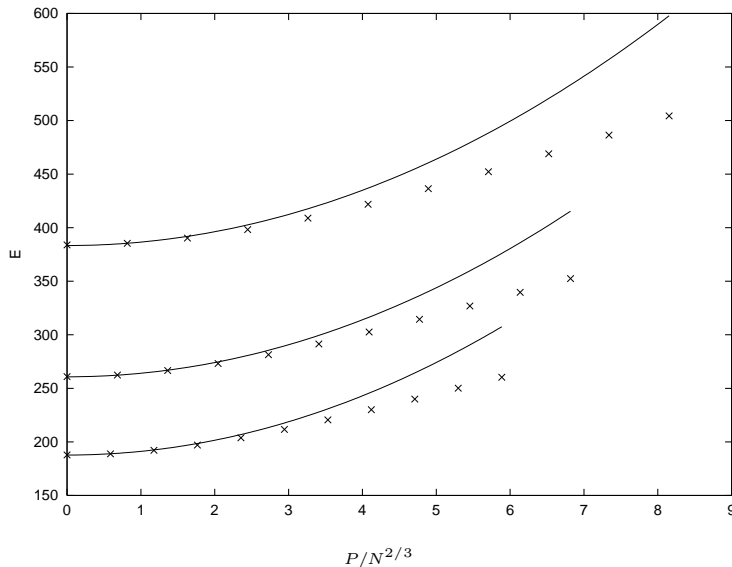


Figure 3: The energy,  $E$ , as a function of the scaled momentum,  $P/N^{2/3}$ , for the three values  $N = 204, 317, 542$ . The crosses represent the numerical data and the curves are obtained from the small momentum approximation.

In figure 3 we plot (crosses) the energy dispersion relation,  $\hat{E}(P, N)$  obtained from these computations for the three values  $N = 204, 317, 542$ . The energy increases with  $N$  so the

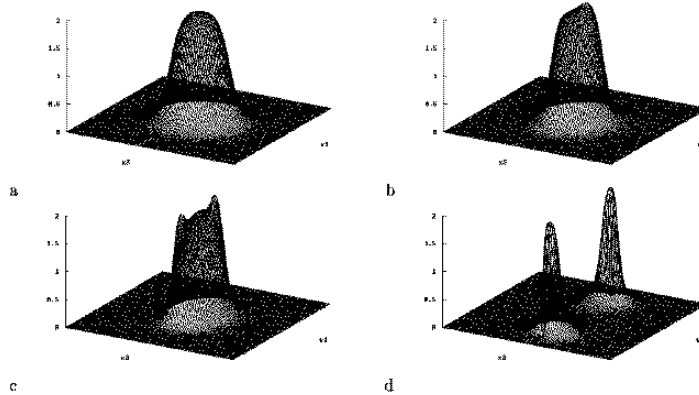


Figure 4: The spin reversal density,  $1 - \phi_3$ , in the  $x_2 = 0$  plane, for the soliton with  $N = 317$ , and four values of the scaled momentum,  $P/N^{2/3} = 0, 6.8, 13.6, 68.2$

data need not be labelled individually. Note that the rather unobvious choice for these three values is due to the fact that in the zero momentum case they correspond to the frequencies  $\omega = 0.7, 0.6, 0.5$ . The soliton velocity, if required, can be read-off from this data by making use of formula (3.2).

We now describe an approximate initial condition for the field  $\phi$  to describe a soliton with any given values of  $N$  and  $P$  and assess its accuracy by computing its energy dispersion relation and comparing with the results displayed in figure 3.

It was noted in ref.[7] that in the two-dimensional case a moving soliton could be generated from initial conditions which consist of performing a space dependent phase transformation on the stationary soliton solution, although no relation was given between the parameter which appears in this transformation and the momentum of the resulting soliton. In the following we study the same type of transformation in the three-dimensional case, although we have a simple explicit form for the parameters  $N, P$  of the corresponding solution and this will allow us to compute the energy dispersion relation to compare with the previous numerical results.

Our approximate initial conditions are given by

$$\phi = \frac{1}{1 + f^2}(2f \cos(Px_3/N), 2f \sin(Px_3/N), 1 - f^2) \quad (3.3)$$

where  $f(r)$  is the stationary soliton profile function with  $N$  spin reversals, which we have already introduced earlier. Note that since  $\phi_3$  is the same as in the stationary case then the number of spin reversals of this field is indeed  $N$ . We now show that the momentum of this field is  $\mathbf{P} = (0, 0, P)$ . By symmetry it is trivial to show that  $P_1 = P_2 = 0$ . Substituting (3.3) into the momentum equation (2.2), using spherical variables and performing the angular

part of the integration we have

$$P_3 = -\frac{16\pi P}{3N} \int_0^\infty \frac{f f' r^3}{(1+f^2)^2} dr = \frac{8\pi P}{N} \int_0^\infty \frac{f^2 r^2}{(1+f^2)} - \frac{1}{3} \left( \frac{f^2 r^3}{(1+f^2)} \right)' dr = P \quad (3.4)$$

where we have used the boundary conditions on  $f(r)$  to set the total derivative term to zero and recognized in the remaining term the expression for  $N$ .

Having verified that this configuration has  $N$  spin reversals and momentum  $P$  we can now compute its energy and derive its dispersion relation. Substituting the field (3.3) into the expression for the energy (1.2) and performing the angular integrals we find

$$E = E_0(N) + P^2 E_1(N), \quad (3.5)$$

where

$$E_0(N) = 8\pi \int_0^\infty \frac{(f'^2 + f^2)r^2}{(1+f^2)^2} dr, \quad E_1(N) = \frac{8\pi}{N^2} \int_0^\infty \frac{f^2 r^2}{(1+f^2)^2} dr \quad (3.6)$$

The dispersion relation obtained from equation (3.5) is also displayed in figure 3 (solid curves) for comparison with the full numerical results. In ref.[3] it is noted that a magnon loop occurs for  $P \gg N^{2/3}$ , and from figure 3 it can be seen that the ansatz is only a good approximation if the momentum stays below this range, since otherwise it begins to lose its accuracy and has considerably more energy than the true solution.

In figure 4 we plot, in the  $x_2 = 0$  plane, the spin reversal density,  $1 - \phi_3$ , for the soliton with  $N = 317$  and four different values of the scaled momentum,  $P/N^{2/3} = 0, 6.8, 13.6, 68.2$

Recall that in the spherical ansatz (3.3) the spin reversal density is assumed to be the same as in the stationary case. Therefore by examining how the spin reversal density changes with increasing momentum we can assess the validity of the ansatz. By a comparison of figures 4a and 4b, it can be seen that the spherical assumption in the ansatz is substantially violated for  $P \sim N^{2/3}$ , with the true soliton being stretched in the plane orthogonal to its motion. For very large momenta,  $P \gg N^{2/3}$ , there is a transition from a single lump of magnons into a magnon loop. Already at  $P/N^{2/3} = 13.6$ , figure 4c, one can see that the soliton is sufficiently distorted so that the maximum of the spin reversal density is no longer on the  $x_3$  axis. For  $P/N^{2/3} = 68.2$ , figure 4d, the soliton has now clearly formed two distinct components, which when we recall the axial symmetry in the  $x_1 x_2$  plane, means that the spin reversal density is now localized around a circle in a plane perpendicular to its motion. In the isotropic case all the solitons have this structure [3] and are known as magnetic vortex rings.

In summary, we have seen that low momentum solitons can be described by a spherical ansatz but as the momentum increases there is a transition from lump-like solitons to ring-like solitons.

## 4 Multi-Soliton Interactions

In this section we discuss the results of a numerical evolution of the full time-dependent Landau-Lifshitz equation (1.3) in order to investigate the interaction and scattering of two solitons.

Two initially stationary and well-separated solitons have an axial symmetry about the line connecting them, and we make use of this symmetry in our numerical evolution code. If we take two solitons on the  $x_3$ -axis, each with momentum only in the  $x_3$  direction, then both the initial conditions and the equations of motion have an axial symmetry in the  $x_1x_2$  plane. We could use cylindrical coordinates and evolve the equations of motion in these variables but this type of implementation can often lead to numerical instabilities associated with coordinate singularities, particularly along the  $x_3$ -axis. We therefore employ the ‘Cartoon’ method recently proposed in ref.[1] in the context of solving the axisymmetric Einstein equations. In this approach the equations are evolved in cartesian coordinates, but on a thin slab, that is the grid has size  $M \times 3 \times M$  so that only 3 points are used in the  $x_2$  direction. In the centre of the slab, which is the plane  $x_2 = 0$ , the equations of motion are evolved in a standard manner; we employ a fourth-order Runge-Kutta method for the time evolution and space derivatives are approximated by second order finite differences. Away from this central slice the field values are determined by making use of the axial symmetry to map to an equivalent point in the central slice,  $x_2 = 0$ . Since the field values in this central slice are only known on a discrete lattice a one-dimensional interpolation algorithm must be employed, which we take to be a simple second order Lagrange interpolant. The results in this section were obtained using grids of size  $M = 201$ , with time and space steps given by  $\Delta t = 0.025$ ,  $\Delta x = 0.3$ .

To obtain an initial condition consisting of two well-separated solitons we use the following nonlinear superposition rule. Given the  $S^2$ -valued field  $\phi$  corresponding to the first soliton we construct the associated Riemann sphere variable obtained by stereographic projection of the  $S^2$ -valued field onto the complex plane. We construct a similar Riemann sphere field for the second soliton and obtain the combined  $S^2$  field by addition of the two Riemann sphere fields followed by an inverse stereographic projection. Note that before the two fields are combined a relative phase,  $\alpha$ , can be introduced corresponding to rotating the  $\phi_1, \phi_2$  components of the first soliton through an angle  $\alpha$ . As we shall see, this relative phase has a marked influence on the force between the two solitons.

As an initial condition we take two solitons, each corresponding to a stationary soliton with  $N = 317$ , placed on the  $x_3$ -axis at the positions  $x_3 = \pm 7$ . Figure 5 displays the subsequent evolution of their relative separation for the cases when there is no relative phase, that is  $\alpha = 0$ , (bottom curve) and when the two solitons are exactly out of phase, that is  $\alpha = \pi$ , (top curve). In computing the separation of the two solitons the position of each soliton is defined as the point at which the spin-reversal density,  $1 - \phi_3$ , takes its maximum value, and this is calculated using a quadratic interpolation around the lattice site at which it takes its maximal value.

From figure 5 we see that when there is no relative phase the two solitons attract and form a single larger soliton, which is perhaps what is expected from the fact that the energy



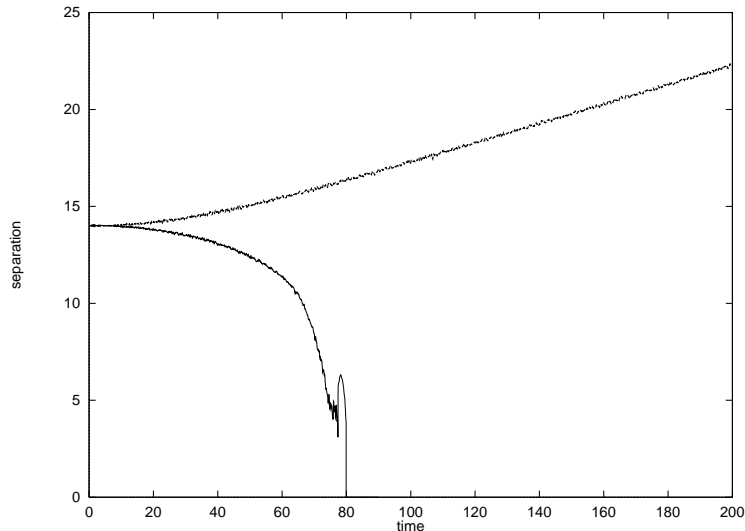


Figure 5: The time evolution of the separation between two initially stationary solitons. The relative internal phase,  $\alpha$ , is set to 0 (bottom curve) and  $\pi$  (top curve).

per spin reversal is a decreasing function of  $N$  as shown in figure 2. The slight peak before the solitons merge in figure 5 is a result of the highly nonlinear deformation the solitons suffer as they combine. In contrast, when the solitons are out of phase they repel and quickly settle to a state in which the two solitons are moving away from each other at a constant speed. Thus we have demonstrated that the force between two solitons can be attractive or repulsive depending on their relative phase.

If the relative phase is something other than 0 or  $\pi$  then the situation is even more complicated. In this case the ultimate fate of the solitons, that is whether the final configuration consists of one or two solitons, depends on the relative phase and initial separation of the solitons. However, the picture is not as simple as a mere attraction or repulsion, as the solitons can initially move towards each other but then turn around and ultimately repel. Furthermore, during this interaction there can be a magnon exchange, so that the number of spin reversals of one soliton can increase while that of the other decreases. Qualitatively similar results have been found and studied in great detail [2] for solitons known as Q-balls, where the role of the number of spin reversals is played by a Noether charge. Q-balls occur in relativistic field theories, in which the dynamics is second order in time, rather than the first order dynamics of the Landau-Lifshitz equation, so it may seem a little surprising that there should be similarities. However, Q-balls have a time-dependent internal phase, very similar to the precession of the magnetization for the magnetic solitons studied in this paper, and as argued in ref.[2], to which we direct the reader for further details, the novel dynamics can be mainly attributed to this fact. As we discuss below, there are other common features between the dynamics of magnetic solitons and Q-balls.

For two solitons which individually have no momentum and are in-phase we have seen

that the two solitons merge and, after some oscillations, settle down to a single soliton which has a value of  $N$  which is approximately the sum of its constituents. A small amount of energy is radiated during these oscillations, in the form of magnons which are released to infinity, and can be dealt with numerically by applying absorbing boundary conditions at the edge of the grid. As we now demonstrate, if the solitons initially have some momentum then a much more complicated evolution takes place.

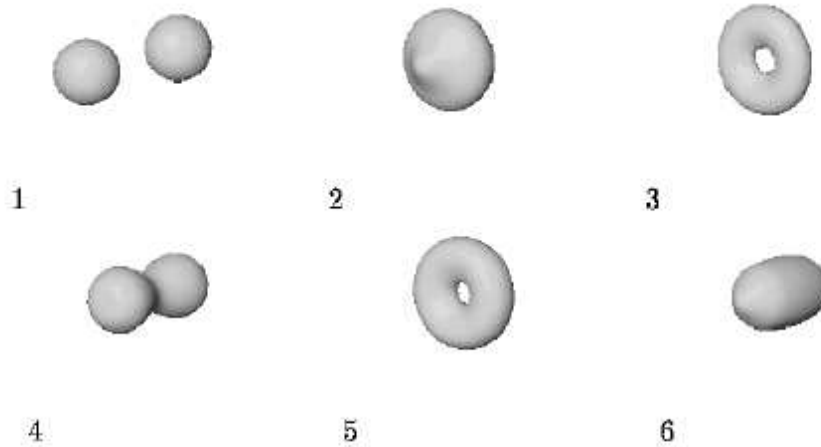


Figure 6: Isosurface plots of  $1 - \phi_3 = 1.5$  at times  $t = 0, 20, 30, 65, 80, 115$  during the collision of two solitons.

In figure 6 we display a fully three-dimensional isosurface plot corresponding to the surface where  $1 - \phi_3 = 1.5$ , at six different times  $t = 0, 20, 30, 65, 80, 115$ . The initial conditions were created from two  $N = 317$  solitons, with zero relative phase, placed at the positions  $x_3 = \pm 7$  and with momentum  $P = \mp 158$ . The individual moving solitons were constructed using the ansatz (3.3), which is an adequate approximation at this momentum. We see from figure 6 that the two solitons collide and form a single lump (figure 6.2) which then expands to form an axially symmetric loop of magnons, that is, a toroidal region where the spin-reversal density is concentrated (figure 6.3). This magnon loop initially expands until it reaches a critical radius, which increases with the initial momentum of the solitons, and then contracts to produce two solitons which move apart along the initial line of approach (figure 6.4). The solitons then attract once more, reforming the loop (figure 6.5), which again collapses, with the solitons again attempting to separate (figure 6.6). This process continues through several cycles, with the loop forming at a slightly smaller radius each time, until eventually the configuration settles to a single large soliton with no momentum. Note that the loop which forms in this process is not the same kind of structure as the moving vortex ring, since it has no momentum perpendicular to the plane of the loop. If the initial momentum of the solitons is increased slightly (for example,

with  $P = 317$ , and all other initial conditions the same) then the first loop formed is of sufficient radius that its collapse results in the two solitons which emerge from its decay having sufficient momentum that they never recombine and instead travel out to infinity.

This phenomenon is the three-dimensional realization of the two-dimensional process described in ref.[7] where two solitons scatter at right angles to the initial line of approach. In the three-dimensional case the axial symmetry prevents the two solitons from scattering at right angles and results instead in the formation of a magnon loop.

This kind of loop formation also appears in relativistic Q-ball dynamics and the qualitative features are very similar [2].

In summary, we have seen that the interaction of multi-solitons, even at relatively low momenta, is a very complicated process with forces which depend on relative internal phases, and novel features such as the production of unstable loops. Clearly these processes require further study and hopefully a more analytical understanding will emerge.

## 5 Conclusion

We have used several different numerical techniques to study the dynamics and interaction of magnetic solitons in a three-dimensional ferromagnet with easy-axis anisotropy. We have computed moving solitons using a minimization algorithm and compared the results to those of a simple radial ansatz, which we have shown is a good approximation for low momenta. However, for large momenta there is a transition from lump-like solitons to ring-like solitons, where obviously the radial ansatz fails badly. We have found that the interaction between two solitons has a strong dependence on their relative phase and that the collision of solitons can be highly non-trivial and lead to the formation of unstable magnon loops. Finally, we have observed that many of the features found for magnetic solitons are qualitatively very similar to those of Q-balls, despite the fact that the dynamics of the latter is a second order in time relativistic system.

## Acknowledgements

We acknowledge the Nuffield Foundation for an award (TI) and the EPSRC for an Advanced Fellowship (PMS).

## References

- [1] M. Alcubierre, S. Brandt, B. Brügmann, D. Holz, E. Seidel, R. Takahashi and J. Thornburg, hep-gr-qc/9908012.
- [2] R.A. Battye and P.M. Sutcliffe, Nucl. Phys. B 590, 329 (2000).
- [3] N.R. Cooper, Phys. Rev. Lett. 82, 1554 (1999).

- [4] M. Hale, O. Schwindt and T. Weidig, Phys. Rev. E 62, 4333 (2000).
- [5] A.M. Kosevich, B.A. Ivanov and A.S. Kovalev, Phys. Rep. 194, 117 (1990).
- [6] N. Papanicolaou and T.N. Tomaras, Nucl. Phys. B 360, 425 (1991).
- [7] B. Piette and W.J. Zakrzewski, Physica D 119, 314 (1998).
- [8] J. Tjon and J. Wright, Phys. Rev. B 15, 3470 (1977).
- [9] P.J.M. van Laarhoven and E.H.L. Aarts, '*Simulated Annealing: Theory and Applications*', Kluwer Academic Publishers (1987).